PHYSICAL REVIEW B **95**, 081304(R) (2017)

Carrier transfer across a 2D-3D semiconductor heterointerface: The role of momentum mismatch

T. Kümmell, U. Hutten, F. Heyer, K. Derr, R.-M. Neubieser, W. Quitsch, and G. Bacher
Werkstoffe der Elektrotechnik and CENIDE, Universität Duisburg-Essen, 47057 Duisburg, Germany
(Received 24 November 2016; published 27 February 2017)

Two-dimensional (2D) transition metal dichalogenides exhibit a unique band structure: In contrast to many direct-gap classical semiconductors, their band-gap minimum is not at the center of the Brillouin zone, but at finite values of the k vector. We report on clear indications that this momentum mismatch fundamentally influences the carrier transfer between a 2D WS_2 crystal and a three-dimensional (3D) GaN layer: Populating different local band extrema of the WS_2 in k space by selective laser excitation leads to a pronounced difference in the WS_2 photoluminescence signal. These findings may be of high importance for future 2D-3D semiconductor devices.

DOI: 10.1103/PhysRevB.95.081304

Atomically thin two-dimensional (2D) materials have become the base for a great variety of nanoscale device concepts [1–4]. Insulating, conducting, and semiconducting materials can be arbitrarily combined without constrictions from lattice symmetries and lattice constants [4]. Meanwhile, van der Waals devices have been designed as transistors [5], light emitters [6,7], photodetectors [2,8], and solar cells [9,10]. The operation of many of these devices implies heterojunctions and therefore an understanding of the carrier transport across these junctions is required [11,12].

However, research is still at an initial state in some respects. While van der Waals materials in principle do not set structural limitations for device designs, one must consider the unique electronic characteristics of the involved materials: The heterojunction physics as known for many years in classical epitaxially fabricated semiconductors cannot be transferred straightforwardly to heterojunctions that include 2D materials. In typical 2D semiconductor monolayers, both conduction and valence band extrema are at the K point in the Brillouin zone, in contrast to most classical direct-gap semiconductors with the band gap at the zone center. On the one hand, this has given rise to various novel magneto-optical effects described by valleytronic physics [13–15]. On the other hand, the finite crystal momentum at the K point might have consequences if different layers are combined: Crystal orientation and therefore the alignment between the 2D building blocks must be taken into account to describe the carrier transport across the interface. This has been done theoretically and experimentally for graphene, hexagonal boron nitride, and a number of semiconducting 2D materials [16–18].

Even more pronounced consequences for the carrier transport across the heterojunction are expected when 2D semiconductors (with a band-gap minimum at the K point) are combined with direct three-dimensional (3D) semiconductors with a band gap at the Γ point. In such heterojunctions, not only are band offsets [19] and doping concentrations [11] expected to play a role, but also the mismatch in crystal momenta between the different materials. Actually, 2D-3D hybrids have gained growing interest for practical applications [20]. First concepts have been pursued for light emitters and photovoltaics, using Si [21,22] or III-V semiconductors [10] as substrates for exfoliated transition metal dichalcogenide (TMDC) flakes. Very recently, even chemical vapor deposition (CVD) growth of TMDCs on GaN has been reported, exploiting the low lattice mismatch between the materials [23,24]. However, the impact of momentum mismatch on carrier transport over the interface and thus the functionality of these novel device architectures have yet to be addressed.

In this Rapid Communication, we use a model system for an experimental access to the role of momentum mismatch on the carrier transfer across a 2D-3D heterointerface, consisting of a monolayer 2D semiconductor with a band gap at the K point and a direct-gap 3D semiconductor with a band gap at the Γ point. In order to monitor the momentum mismatch, one has to be aware that the band structure of TMDCs such as WS_2 opens a pathway to control the carrier population in k space not only by carrier injection [25,26] but also by the excitation wavelength [27]. This is illustrated in Figs. 1(a) and 1(b). It has been shown that in addition to the WS_2 absorption maxima at 2.1 and 2.4 eV, attributed to the A and B excitons, respectively, a third significant absorption is found in the regime between 2.8 and 3.1 eV [28,29]. Excitation in this energy range (i.e., excitation in the blue spectral range) stimulates the buildup of the C exciton, i.e., the generation of carriers between the Λ point and the Γ point in k space [27,28,30]. Fast thermal relaxation is expected to result in an intermediate state with an increased electron population at the Λ point and hole population at the Γ point [27] [Fig. 1(a)]. This situation is in strong contrast to excitation with lower energies between 2.3 and 2.4 eV (green spectral range) that immediately leads to a population of the K point both in the conduction and valence bands [Fig. 1(b)] of the WS_2. In a 2D-3D heterostructure, the different excitation conditions are expected to have consequences for the carrier transfer: While after excitation of WS_2 near the Γ point a transfer to the 3D GaN substrate is possible with respect to the crystal momentum [Fig. 1(c)], it may be hampered after excitation near the K point [Fig. 1(d)].

From these considerations, we develop our experiment as follows: Exfoliated WS_2 monolayers represent the 2D semiconductor. Three different substrate types were investigated: (i) Si/SiO_2, (ii) i-GaN, and (iii) p-GaN (doping density $>10^{18}/cm^3$). Flakes on Si/SiO_2 serve as a reference, because on these insulating substrates no carrier transfer whatsoever is expected because of the huge SiO_2 band gap. GaN serves as a 3D semiconductor. A wide-gap semiconductor such as GaN makes sure that carriers under excitation with visible light are photogenerated solely in the 2D material. Reported affinities for WS_2 range from 3.9 to 4.5 eV [31,32], and for GaN the values given are between 3.5 and 4.1 eV [33,34]. Therefore,

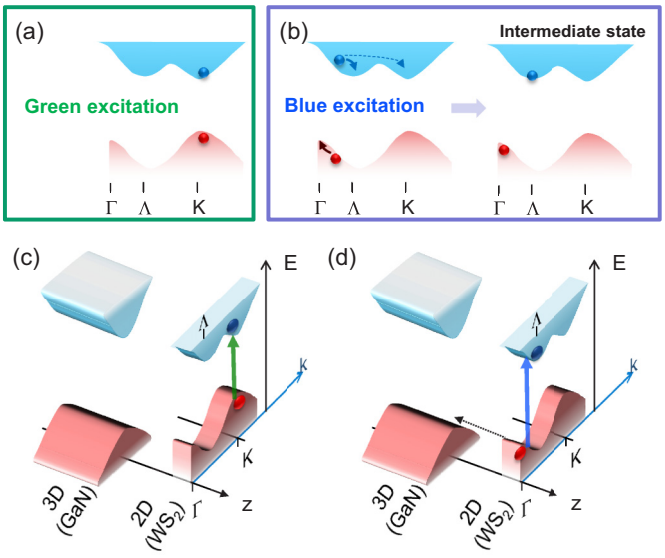

FIG. 1. Carrier population in WS_2 after excitation with photon energies (a) slightly larger than the band gap (green excitation) and (b) significantly larger than the band gap (blue excitation). (c), (d) Expected consequences for a carrier transfer from WS_2 to a 3D semiconductor (GaN) substrate.

this system principally represents a type I heterojunction and a carrier transfer from the 2D to the 3D semiconductor should be prohibited for energetic reasons. However, the doping of GaN will change the alignment between the bands in 2D and 3D semiconductors, thus modifying carrier transfer from the 2D semiconductor. In the case of a *p*-doped 3D semiconductor, a transfer of holes from WS_2 to GaN can be enabled (see Fig. 2). To countercheck this substrate influence, stacked structures with hexagonal boron nitride (hBN) between WS_2 and *p*-GaN were realized as well. These structures were fabricated by first exfoliating hBN directly on *p*-GaN. Subsequently, WS_2 was exfoliated on a transparent polydimethylsiloxan (PDMS) stamp [35], aligned by micromanipulators under an optical microscope with the hBN flakes and finally transferred.

At these 2D-3D hybrids, we use microphotoluminescence spectroscopy to study the carrier transfer from the 2D to 3D semiconductor dependent on excitation in *k* space, i.e., we excite with two different wavelengths: $\lambda = 532\,\text{nm}$ for excitation near the *K* point and $\lambda = 405\,\text{nm}$ for excitation near the Γ point. Photoluminescence (PL) measurements were made by a commercial confocal PL setup (NT-MDT Ntegra) at room temperature. This setup enables us to perform PL mappings with a spatial resolution down to 300 nm, which will become important for stacked structures including hBN.

In Fig. 2(a), room temperature photoluminescence spectra of monolayer WS_2 are depicted for different substrates and for two different excitation wavelengths. The excitation power of $300\,\mu\text{W}$ corresponds to an excitation density of approximately $200\,\text{kW/cm}^2$. The spectra are not normalized, but shifted vertically for clarity; the intensity is marked by the vertical scale bar. We obtain a striking difference between the photoluminescence by changing the excitation wavelength. At green excitation ($\lambda = 532\,\text{nm}$) the photoluminescence is virtually independent of the substrate. The PL maximum at 2.08 eV can be attributed to the exciton at the band edge, i.e., at the *K* point of the Brillouin zone. The low-energy shoulder is due to trionic recombination that is apparent in WS_2 even at room temperature [36]. From this data, we conclude that no significant carrier transfer to the substrate is present. This is well known for the insulating Si/SiO_2 substrate. For the GaN substrate it confirms that WS_2/GaN is a type I heterostructure.

With blue excitation ($\lambda = 405\,\text{nm}$), a completely different behavior is found. On the insulating substrates (SiO_2 and *i*-GaN), the excitonic recombination is observed again, with a stronger trionic component than under green excitation. In contrast, on the *p*-doped GaN substrate, the luminescence is virtually quenched. This is especially remarkable, as only small intensity deviations are found for the other measurements.

In the following, we will show that this result can be explained by taking into account that photoexcitation with blue light carriers is generated close to the Γ point, as illustrated in Figs. 1(a) and 1(c). When discussing the recombination process, it is important to remember that, in contrast to bilayers,

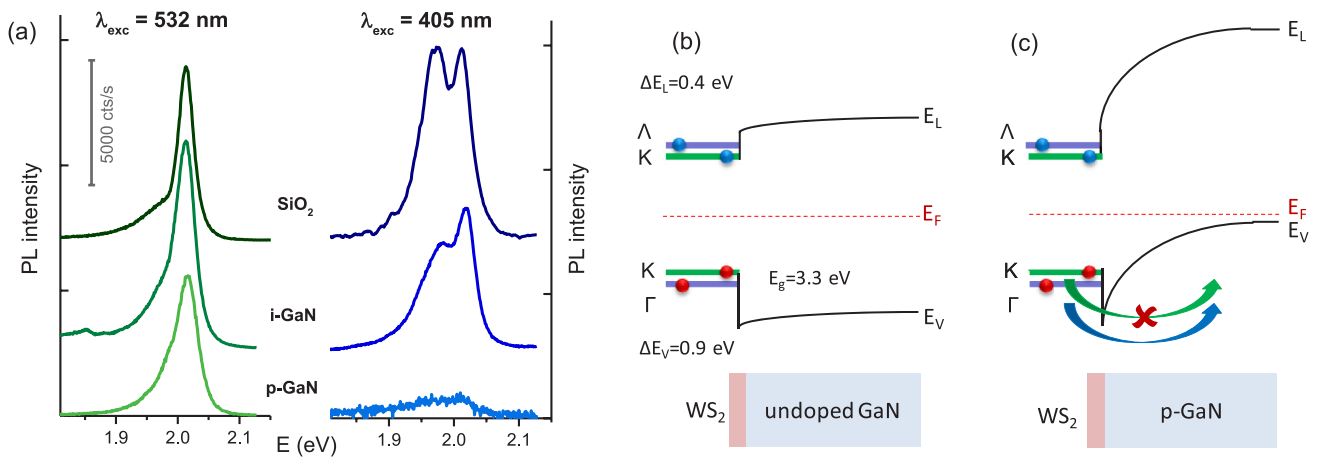

FIG. 2. (a) Photoluminescence spectra of WS_2 monolayer flakes on different substrates under excitation with green light (left) and blue light (right). (b) Scheme of the band structure of the heterojunction between a WS_2 monolayer and *i*-GaN. (c) Scheme of the band structure of the heterojunction between a WS_2 monolayer and *p*-GaN. Qualitatively, the depletion area in GaN is included in the figure.

no indirect Λ-Γ transition is observed in the monolayers, because the lowest energy is found for the K-K transition. Thus, the population of the Λ minimum (Γ maximum) with electrons (holes) is an intermediate state and intervalley scattering will finally lead to a population of the K extrema in the conduction and valence band, followed by recombination that becomes visible as the A transition [27]. This is the situation usually described in the literature, where WS_2 is placed on an insulator such as SiO_2, in agreement with our findings [see Fig. 2(a)]. When choosing i-GaN as a substrate, with the Fermi energy E_F near the band-gap center for both materials, the heterojunction can be sketched as illustrated in Fig. 2(b), where both the K-K population after green excitation and the Λ-Γ population after blue excitation are schematically indicated. From literature data [31–34], we assume that the band offsets in the conduction bands will be smaller than in the valence bands; in our viewgraph we chose $\Delta E_C = 0.4\,\text{eV}$ for the conduction band and $\Delta E_V = 0.9\,\text{eV}$ for the valence band offset. The energy difference between K and Γ electrons and holes was taken as 0.15 and 0.2 eV, respectively [37]. Obviously, both electrons and holes are confined to the 2D semiconductor flake due to its narrower band gap, independent of the excitation energy. This is confirmed by our experiment, where a pronounced WS_2 PL signal is observed and no significant difference in intensity is found between blue and green excitation. A point to note is the slightly stronger trionic component that is observed under blue excitation. This finding principally confirms the idea that under these conditions holes are predominantly excited close to the Γ maximum, leading to a lack of holes at the K point and therefore to negative trion recombination.

By using p-doped GaN we are opening a channel for possible carrier loss, as indicated in Fig. 2(c). Assuming the depletion zone to be located in p-GaN, holes generated optically within WS_2 (note the excitation wavelength chosen does not allow one to create electron-hole pairs in GaN) principally can be transferred to the valence band of p-GaN, whereas the electrons are expected to be confined to the 2D semiconductor. Our observations show that the PL signal of WS_2 on p-GaN exhibits a similar intensity as WS_2 on top of a SiO_2 or an i-GaN substrate after green excitation, while the PL signal of WS_2 on top of p-GaN is completely quenched in the case of blue excitation [see Fig. 2(a)]. Obviously there is a fundamental difference between holes at the Γ point (generated in the case of blue excitation) and holes at the K point (generated for green excitation): While in the first case, i.e., for holes at the Γ point of the valence band in WS_2, transfer across the 2D-3D heterointerface is apparently quite efficient, in the latter case (holes at the K point in WS_2) the holes are kept confined to the 2D semiconductor.

Hereby, we have to consider that the hole wave function is strongly confined to the W cations for K holes and electrons in monolayers, while carriers with smaller k vectors, i.e., at or near the Γ point, exhibit wave functions expanding in the vicinity [38]. Thus, in the latter case, a stronger interaction of the holes in the WS_2 with the GaN substrate or with interface states is expected. In addition, and probably even more important, K holes are bearing a strongly different crystal momentum compared to holes at the Γ point. Before being transferred from the K point of the WS_2 to the Γ point of the GaN substrate, the carriers have to lose this momentum by scattering at defects or interface states. As a consequence, this scattering process has to compete with the fast (on the order of ps) carrier recombination [39] at the K point, strongly suppressing 2D-3D hole transfer. We thus interpret our findings as a clear hint of the role of momentum mismatch for the carrier transfer across 2D-3D heterointerfaces. Holes at the Γ point (i.e., after blue excitation) have to be scattered to the K point before they can recombine with electrons, while a transfer to the 3D substrate is possible without momentum change, enhancing the probability for the latter process.

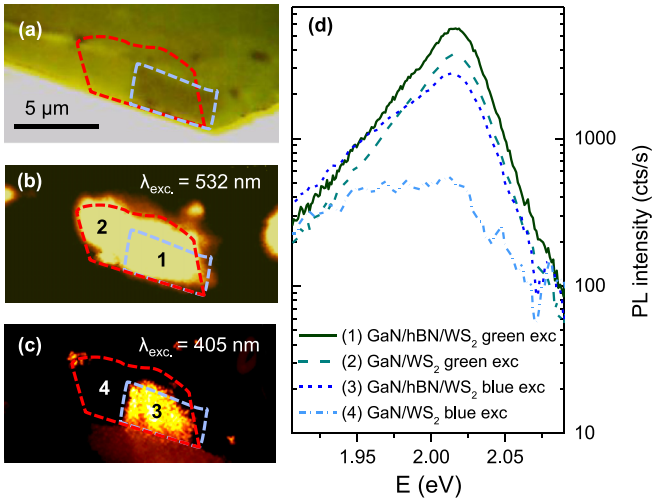

FIG. 3. Stacked GaN/hBN/WS_2 structures. (a) Optical microscope image. (b) PL map under green excitation. (c) PL map under blue excitation. The monolayer area is marked red and the hBN light blue. (d) PL spectra from the areas marked by numbers in (b) and (c).

In order to demonstrate the substrate influence within one flake, we fabricated stacked WS_2/hBN/p-GaN van der Waals heterostructures, where a part of the WS_2 flake is separated from the p-GaN substrate by an isolating layer. Hexagonal boron nitride (hBN) flakes have been exfoliated on p-doped GaN in order to serve as an ultrathin insulating barrier. The hBN flake thickness was quantified to 8 nm by atomic force microscopy. Note that a sufficient thickness is necessary to prevent tunneling over hBN [6,40]. A larger WS_2 monolayer flake was positioned on top of the hBN flake, being partially in direct contact with the p-GaN substrate and partially on the surface of the insulating hBN.

While under optical microscopy the contrasts are quite low [Fig. 3(a)], photoluminescence maps under excitation at $\lambda = 532\,\text{nm}$ reveal the monolayer regions very clearly [Fig. 3(b)]. Only a small difference in the absolute PL intensity is observed for the WS_2/p-GaN and the WS_2/hBN/p-GaN areas, which we attribute to a partial suppression of nonradiative surface losses due to hBN, in agreement with literature [6]. In contrast, mapping with $\lambda = 405\,\text{nm}$ shows a significantly smaller luminescent zone that coincides very well with the position of the hBN/WS_2 stacks [Fig. 3(c)]. The luminescence in the areas where WS_2 is in direct contact with p-GaN is strongly suppressed, in agreement with the data shown before [Fig. 2(a)]. A comparison of the PL spectra [Fig. 3(d)] shows nearly equal luminescence

intensities for blue and green excitation in the case of the WS_2/hBN/p-GaN stacks. The thin hBN layer obviously prevents a carrier loss to the p-doped substrate, independent from the excitation condition. This is expected for an insulator and confirms again that the luminescence loss under blue excitation is most likely attributed to carrier transfer to the 3D semiconductor.

In conclusion, 2D-3D semiconductor heterojunctions are studied by wavelength-selective optical excitation. Our results suggest that carrier transfer across the 2D-3D heterointerface significantly depends on the excitation conditions, i.e., the k vector of the carriers optically generated in the 2D semiconductor. Momentum mismatch between the holes at the K point in the WS_2 and the Γ point in the semiconducting p-GaN substrate strongly suppresses carrier transfer across the interface, while Γ holes can apparently escape efficiently from the 2D to the 3D semiconductor, quenching the WS_2 PL signal after blue excitation. This hole transfer can be blocked by inserting a thin layer of hBN. These findings seem to be highly important for the layout of future optoelectronic 2D-3D heterojunction devices, such as wavelength-selective detectors or filters.

[1] J. S. Ross, P. Klement, A. M. Jones, N. J. Ghimire, J. Q. Yan, D. G. Mandrus, T. Taniguchi, K. Watanabe, K. Kitamura, W. Yao, D. H. Cobden, and X. D. Xu, Nat. Nanotechnol. **9**, 268 (2014).

[2] C.-H. Lee, G.-H. Lee, A. M. Van Der Zande, W. Chen, Y. Li, M. Han, X. Cui, G. Arefe, C. Nuckolls, T. F. Heinz, J. Guo, J. Hone, and P. Kim, Nat. Nanotechnol. **9**, 676 (2014).

[3] F. Xia, H. Wang, D. Xiao, M. Dubey, and A. Ramasubramaniam, Nat. Photonics **8**, 899 (2014).

[4] A. K. Geim and I. V. Grigorieva, Nature (London) **499**, 419 (2013).

[5] B. Radisavljevic, A. Radenovic, J. Brivio, V. Giacometti, and A. Kis, Nat. Nanotechnol. **6**, 147 (2011).

[6] F. Withers, O. Del Pozo-Zamudio, S. Schwarz, S. Dufferwiel, P. M. Walker, T. Godde, A. P. Rooney, A. Gholinia, C. R. Woods, P. Blake, S. J. Haigh, K. Watanabe, T. Taniguchi, I. L. Aleiner, A. K. Geim, V. I. Fal'ko, A. I. Tartakovskii, and K. S. Novoselov, Nano Lett. **15**, 8223 (2015).

[7] W. Yang, J. Shang, J. Wang, X. Shen, B. Cao, N. Peimyoo, C. Zou, Y. Chen, Y. Wang, C. Cong, W. Huang, and T. Yu, Nano Lett. **16**, 1560 (2016).

[8] L. Britnell, R. M. Ribeiro, A. Eckmann, R. Jalil, B. D. Belle, A. Mishchenko, Y.-J. Kim, R. V. Gorbachev, T. Georgiou, S. V. Morozov, A. N. Grigorenko, A. K. Geim, C. Casiraghi, A. H. C. Neto, and K. S. Novoselov, Science **340**, 1311 (2013).

[9] F. Wang, Z. X. Wang, K. Xu, F. M. Wang, Q. S. Wang, Y. Huang, L. Yin, and J. He, Nano Lett. **15**, 7558 (2015).

[10] S. S. Lin, P. Wang, X. Q. Li, Z. Q. Wu, Z. J. Xu, S. J. Zhang, and W. L. Xu, Appl. Phys. Lett. **107**, 153904 (2015).

[11] M. Massicotte, P. Schmidt, F. Vialla, K. G. Schädler, A. Reserbat-Plantey, K. Watanabe, T. Taniguchi, K. J. Tielrooij, and F. H. L. Koppens, Nat. Nanotechnol. **11**, 42 (2016).

[12] X. P. Hong, J. Kim, S. F. Shi, Y. Zhang, C. H. Jin, Y. H. Sun, S. Tongay, J. Q. Wu, Y. F. Zhang, and F. Wang, Nat. Nanotechnol. **9**, 682 (2014).

[13] K. F. Mak, K. L. McGill, J. Park, and P. L. Mceuen, Science **344**, 1489 (2014).

[14] A. M. Jones, H. Yu, N. J. Ghimire, S. Wu, G. Aivazian, J. S. Ross, B. Zhao, J. Yan, D. G. Mandrus, D. Xiao, W. Yao, and X. Xu, Nat. Nanotechnol. **8**, 634 (2013).

[15] G. Sallen, L. Bouet, X. Marie, G. Wang, C. R. Zhu, W. P. Han, Y. Lu, P. H. Tan, T. Amand, B. L. Liu, and B. Urbaszek, Phys. Rev. B **86**, 081301 (2012).

[16] S. Huang, X. Ling, L. Liang, J. Kong, H. Terrones, V. Meunier, and M. S. Dresselhaus, Nano Lett. **14**, 5500 (2014).

[17] B. Hunt, J. D. Sanchez-Yamagishi, A. F. Young, M. Yankowitz, B. J. Leroy, K. Watanabe, T. Taniguchi, P. Moon, M. Koshino, P. Jarillo-Herrero, and R. C. Ashoori, Science **340**, 1427 (2013).

[18] H. Heo, J. H. Sung, S. Cha, B.-G. Jang, J.-Y. Kim, G. Jin, D. Lee, J.-H. Ahn, M.-J. Lee, J. H. Shim, H. Choi, and M.-H. Jo, Nat. Commun. **6**, 7372 (2015).

[19] J. Kang, S. Tongay, J. Zhou, J. Li, and J. Wu, Appl. Phys. Lett. **102**, 012111 (2013).

[20] D. Jariwala, T. J. Marks, and M. C. Hersam, Nat. Mater. **16**, 170 (2017).

[21] M.-L. Tsai, S.-H. Su, J.-K. Chang, D.-S. Tsai, C.-H. Chen, C.-I. Wu, L.-J. Li, L.-J. Chen, and J.-H. He, ACS Nano **8**, 8317 (2014).

[22] B. Li, G. Shi, S. Lei, Y. He, W. Gao, Y. Gong, G. Ye, W. Zhou, K. Keyshar, J. Hao, P. Dong, L. Ge, J. Lou, J. Kono, R. Vajtai, and P. M. Ajayan, Nano Lett. **15**, 5919 (2015).

[23] S. M. Eichfeld, L. Hossain, Y.-C. Lin, A. F. Piasecki, B. Kupp, A. G. Birdwell, R. A. Burke, N. Lu, X. Peng, J. Li, A. Azcatl, S. McDonnell, R. M. Wallace, M. J. Kim, T. S. Mayer, J. M. Redwing, and J. A. Robinson, ACS Nano **9**, 2080 (2015).

[24] Z. Chen, H. Liu, X. Chen, G. Chu, S. Chu, and H. Zhang, ACS Appl. Mater. Interfaces **8**, 20267 (2016).

[25] Z. Li, G. Ezhilarasu, I. Chatzakis, R. Dhall, C.-C. Chen, and S. B. Cronin, Nano Lett. **15**, 3977 (2015).

[26] T. Kümmell, W. Quitsch, S. Matthis, T. Litwin, and G. Bacher, Phys. Rev. B **91**, 125305 (2015).

[27] D. Kozawa, R. Kumar, A. Carvalho, K. Kumar Amara, W. Zhao, S. Wang, M. Toh, R. M. Ribeiro, A. H. Castro Neto, K. Matsuda, and G. Eda, Nat. Commun. **5**, 2992 (2015).

[28] H. M. Hill, A. F. Rigosi, C. Roquelet, A. Chernikov, T. C. Berkelbach, D. R. Reichman, M. S. Hybertsen, L. E. Brus, and T. F. Heinz, Nano Lett. **15**, 2992 (2015).

[29] W. Zhao, Z. Ghorannevis, L. Chu, M. Toh, C. Kloc, P.-H. Tan, and G. Eda, ACS Nano **7**, 791 (2013).

[30] D. Y. Qiu, F. H. da Jornada, and S. G. Louie, Phys. Rev. Lett. **111**, 216805 (2013).

[31] S. Hwan Lee, D. Lee, W. Sik Hwang, E. Hwang, D. Jena, and W. Jong Yoo, Appl. Phys. Lett. **104**, 193113 (2014).

[32] C. Gong, H. Zhang, W. Wang, L. Colombo, R. M. Wallace, and K. Cho, Appl. Phys. Lett. **103**, 053513 (2013).

[33] G. Koley and M. G. Spencer, J. Appl. Phys. **90**, 337 (2001).

[34] Y. Hinuma, A. Grüneis, G. Kresse, and F. Oba, Phys. Rev. B **90**, 155405 (2014).
[35] K. Choi, Y. T. Lee, S.-W. Min, H. S. Lee, T. Nam, H. Kim, and S. Im, J. Mater. Chem. C **1**, 7803 (2013).
[36] G. Plechinger, P. Nagler, J. Kraus, N. Paradiso, C. Strunk, C. Schuller, and T. Korn, Phys. Status Solidi RRL **9**, 457 (2015).
[37] H. Zeng, G.-B. Liu, J. Dai, Y. Yan, B. Zhu, R. He, L. Xie, S. Xu, X. Chen, W. Yao, and X. Cui, Sci. Rep. **3**, 1608 (2013).
[38] L. Zhang and A. Zunger, Nano Lett. **15**, 949 (2015).
[39] D. Lagarde, L. Bouet, X. Marie, C. R. Zhu, B. L. Liu, T. Amand, P. H. Tan, and B. Urbaszek, Phys. Rev. Lett. **112**, 047401 (2014).
[40] G.-H. Lee, Y.-J. Yu, C. Lee, C. Dean, K. L. Shepard, P. Kim, and J. Hone, Appl. Phys. Lett. **99**, 243114 (2011).